

The PRRT2 knockout mouse recapitulates the neurological diseases associated with *PRRT2* mutations

Caterina Michetti^a, Enrico Castroflorio^{a,b}, Ivan Marchionni^a, Nicola Forte^a, Bruno Sterlini^b, Francesca Binda^a, Floriana Fruscione^c, Pietro Baldelli^{a,b}, Flavia Valtorta^d, Federico Zara^c, Anna Corradi^a and Fabio Benfenati^{a,b}

^aCenter for Synaptic Neuroscience and Technology, Istituto Italiano di Tecnologia, Largo Rosanna Benzi 10, 16132 Genova, Italy; ^bDepartment of Experimental Medicine, University of Genova, Viale Benedetto XV, 3, 16132 Genova, Italy; ^cDepartment Head and Neck Neuroscience, Laboratory of Neurogenetics and Neuroscience, Institute G. Gaslini, Via Gerolamo Gaslini, 5, 16148 Genova, Italy; ^dSan Raffaele Scientific Institute and Vita Salute University, Via Olgettina 58, 20132 Milano, Italy.

SUPPLEMENTARY MATERIALS

LEGENDS TO THE SUPPLEMENTARY FIGURES AND MOVIES

Figure S1. Molecular characterization of the PRRT2 KO mice

A. Schematic representation of *Prrt2* wild type locus and of the EUCOMM/KOMP targeted KO-first PRRT2 allele with the targeting cassette inserted between Exon 1 and 2 of *Prrt2* wild type locus. The targeting cassettes include an Engrailed splice acceptor site (En2 SA), an IRES LacZ gene and a promoter driven neomycin resistance cassette (neo) flanked by LoxP sites. The position of PCR primers for genotyping is indicated. **B.** Representative PCR analysis of tail genomic DNA from WT, HET and KO mice confirming the insertion of the targeting construct between the Exons 1 and 2 of the PRRT2 wild type locus. **C.** The regional expression of PRRT2 protein is widespread in the CNS. *Left:* Representative images of PRRT2 immunoblotting in WT (upper panel), HET (middle panel) and KO (lower panel). Calnexin was used as a housekeeping gene for PRRT2 normalization. *Right:* The histogram shows the normalized PRRT2 immunoreactivity in various brain regions (FCX: frontal cortex; SCX: somatosensory cortex; VCX: visual cortex; HIP: hippocampus; STR: striatum; OB: olfactory bulb; BS: brainstem; CB: cerebellum). All data are expressed as means \pm SEM; ** $p < 0.01$, *** $p < 0.001$; one-way ANOVA and post-hoc Bonferroni's test. N = 3 for both WT and KO mice.

Figure S2. Gross histology of the hippocampus and cerebellum.

A. Representative confocal images of the hippocampus (-1.70 from Bregma) of WT and PRRT2 KO mice stained with NeuN (green) and morphometric analysis of the thickness of the pyramidal layer and stratum radiatum of CA1 and CA3 and of the granular and molecular layers of the DG. **B.** Representative confocal images of the lobes IV/V of the cerebellum of WT and PRRT2 KO mice (Lateral 2.04 mm) and morphometric analysis of the thickness of the molecular and granule cell layers. Data are expressed as means \pm SEM. Two-tailed unpaired Student's *t*-test. N = 3 for both WT and KO mice. Scale bar, 150 μ m.

Figure S3. Motor behavioral patterns of PRRT2 KO mice in the open field.

A. Representative tracking of locomotor activity performed by WT, HET and KO mice. **B-E.** Duration of grooming (**B**) and locomotion (**C**), number of entries to the center (**D**), time spent in the borders versus time spent in the center (**E**), by WT, HET and KO male mice during the 20-min open field test. Data are expressed as means \pm SEM. Two-way ANOVA and post-hoc Fisher PLSD test. N = 8 WT, 14 HET and 13 KO mice.

Figure S4. Motor coordination and gait are not affected in PRRT2 KO mice

A. Schematic panel of foot print test: Stride length (SL) calculated as vertical distance between hind paws; Fore-Base width (FBW) calculated as distance between fore paws, Hind-Base Width (HBW) calculated as distance between hind paws. **B.** Latency to fall from an accelerated Rotarod in WT, HET and KO adult male mice. **C-E.** Assessment of gait using Stride length (SL; **C**), Fore base width (FBW; **D**) and Hind base width (HBW; **E**). Data are expressed as means \pm SEM. Two-way ANOVA and post-hoc Fisher PLSD test. N = 8 WT, 14 HET and 13 KO mice.

Figure S5. Novel object recognition is not altered in PRRT2 KO mice

Time of exploration of two objects during the familiarizations phase (**A**) and time of exploration of one familiar object vs a novel object (**B**) performed by WT, HET and KO mice. Data are expressed as means \pm SEM. * $p < 0.05$; two-way ANOVA and post-hoc Fisher PLSD test. N = 12 WT, 18 HET and 10 KO male mice.

Figure S6. Contextual and cued fear conditioning is not impaired in PRRT2 KO mice

Duration of freezing behavior performed by WT, HET and KO mice during the conditioning phase (**A**), contextual test (**B**) and cued test (**C**). Data are expressed as means \pm SEM. Two-way ANOVA and post-hoc Fisher PLSD test. N = 12 WT, 18 HET and 10 KO male mice.

Figure S7. Expression of synaptic markers in the molecular layer of the dentate gyrus in PRRT2 KO mice

Representative confocal images of the molecular layer of the DG of WT and PRRT2-KO mice stained with DAPI (blue), VGAT (green), VGLUT1 (red) and their merge. Histograms on the right show the mean intensity VGAT and VGLUT1 immunoreactivities and the number of VGAT- and VGLUT1-positive puncta. (ML: molecular layer; GL: granule cell layer). Data are expressed as means \pm SEM. Scale bar, 150 μ m.

Figure S8. High-frequency depression is not altered in the PRRT2 KO dentate gyrus

Right: Mean (\pm SEM) normalized values of eEPSC (A) and eIPSC (B) amplitude showing the time course of synaptic depression in GCs subjected to 2-s high-frequency stimulation at 40 Hz. *Left:* Representative traces showing synchronous EPSCs and eIPSCs evoked by the tetanic stimulation. Two-tailed unpaired Student's *t*-test. N = 13 and 12 neurons from WT (4 mice) and PRRT2 KO (4 mice), respectively.

Movie S1. Back walking locomotion of PRRT2 KO mice during spontaneous motor activity

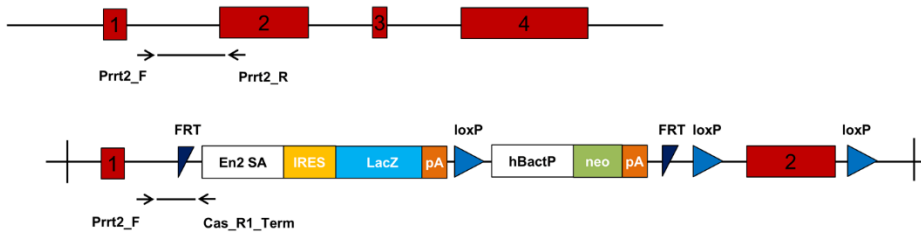
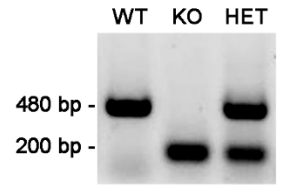
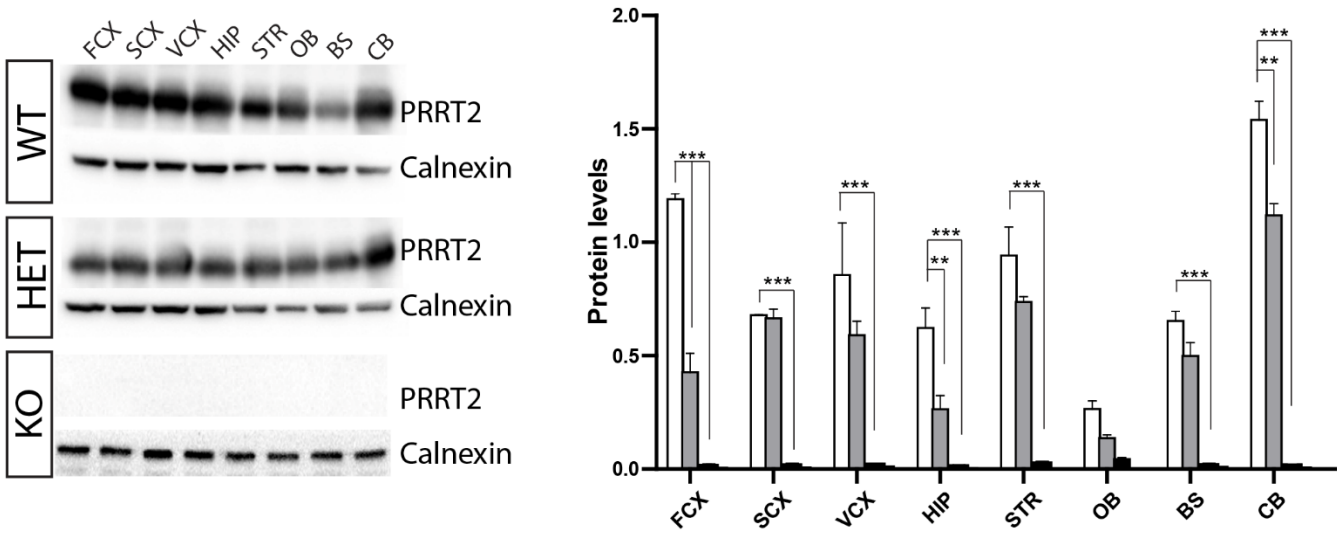
The video depicts the spontaneous motor activity of an adult PRRT2 KO mouse tested in an open field and showing episodes of backward locomotion.

Movie S2. Lack of response of WT mice to an audiogenic stimulus

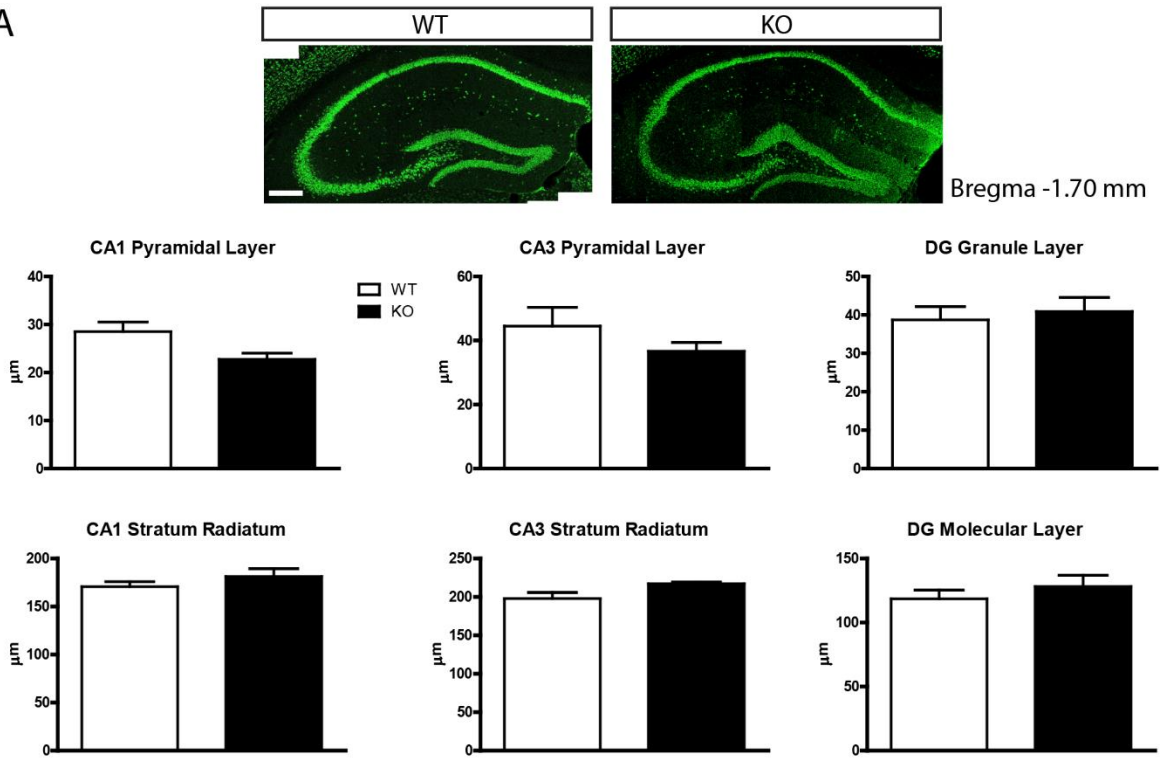
The video depicts an adult WT mouse challenged with a single 120 dB white tone for 60 s. None of the WT (or HET) mice presented sound-induced audiogenic seizures.

Movie S3. Locomotor response of PRRT2 KO mice to audiogenic stimuli

The video depicts an adult PRRT2 KO mouse challenged with a single 120 dB white tone for 60 s. All PRRT2 KO mice presented sound-induced audiogenic seizures consisting in wild, explosive running episodes often accompanied by back walking and jumping.

A**B****C****Figure S1**

A



B

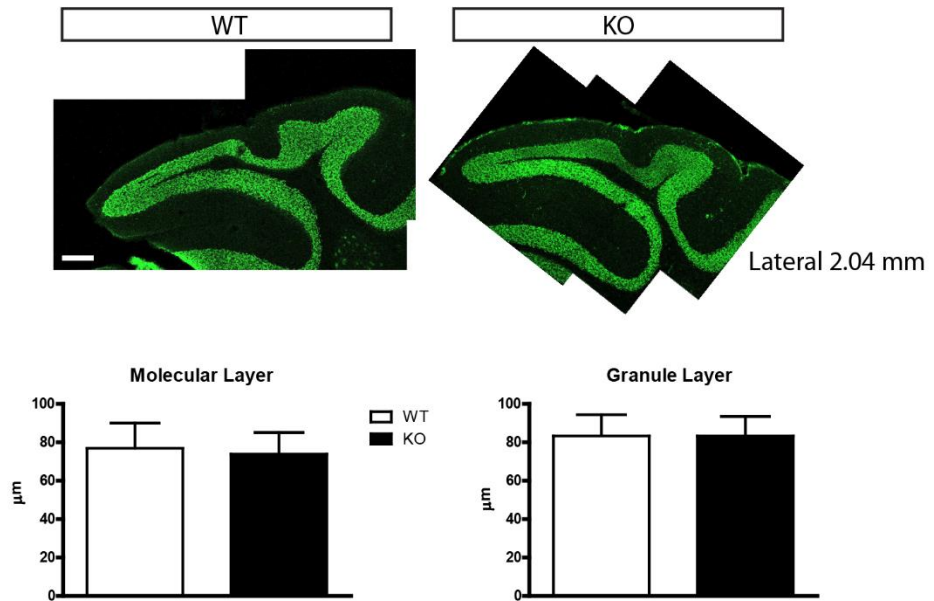


Figure S2

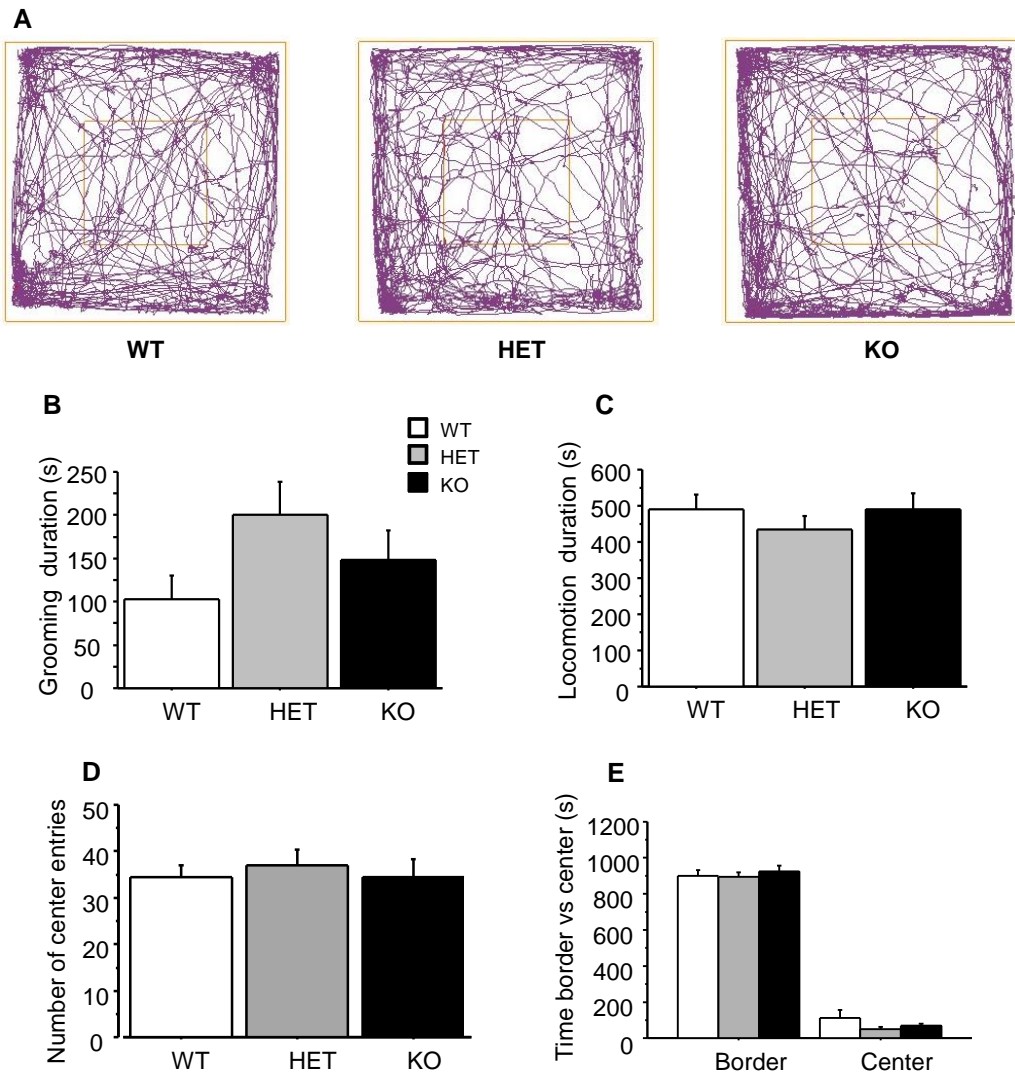


Figure S3

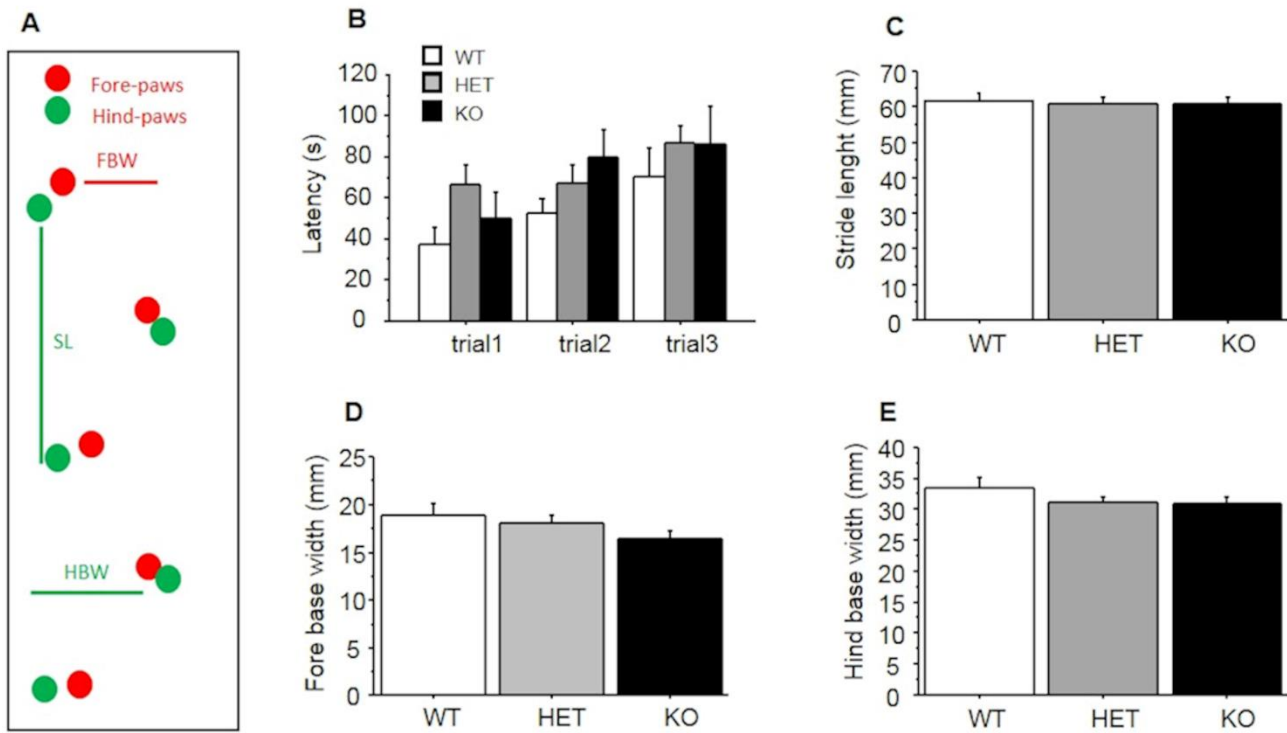


Figure S4

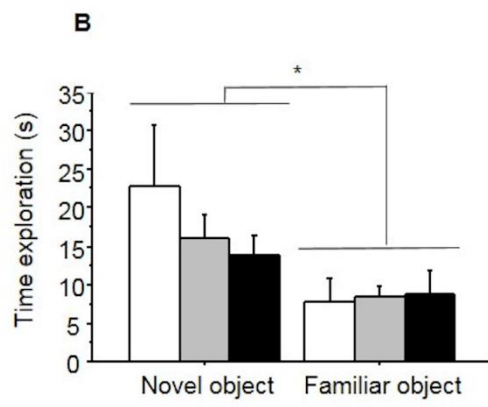
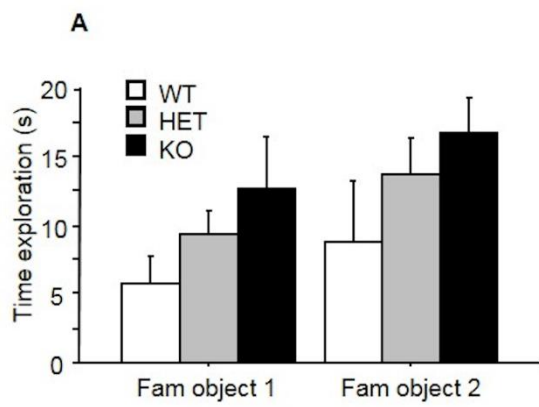
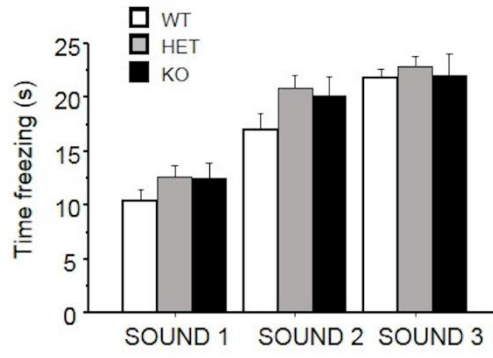
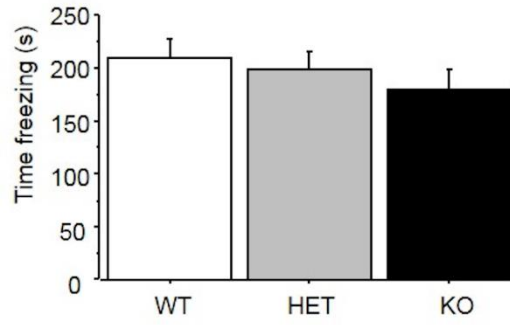


Figure S5

A *CONDITIONING (SOUND+SHOCK)*



B *CONTEXT*



C *CUE*

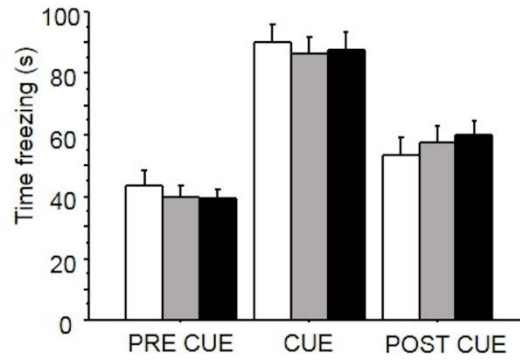


Figure S6

DENTATE GYRUS

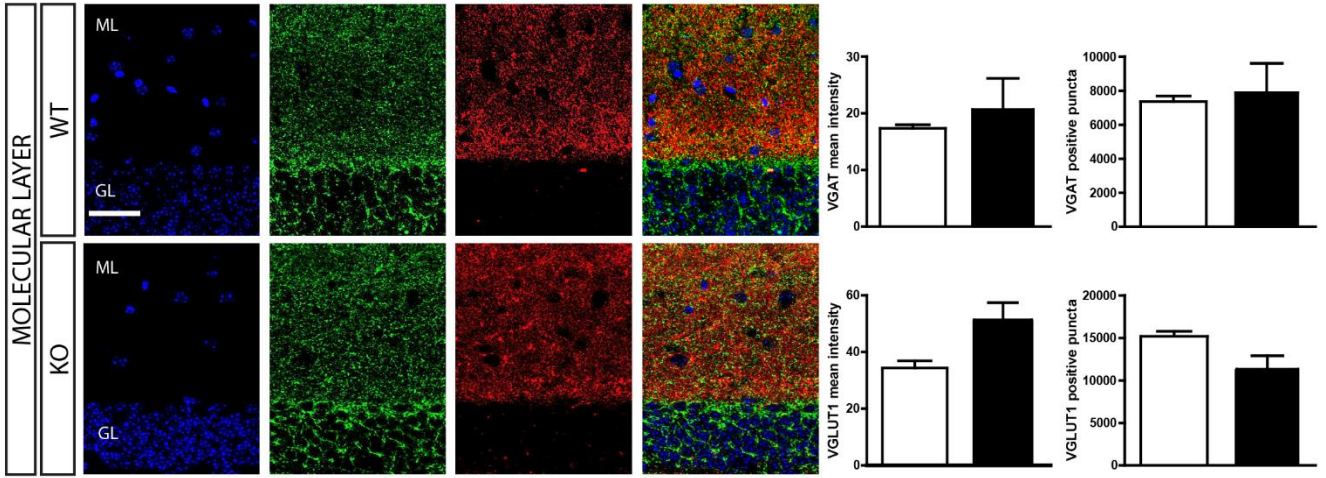


Figure S7

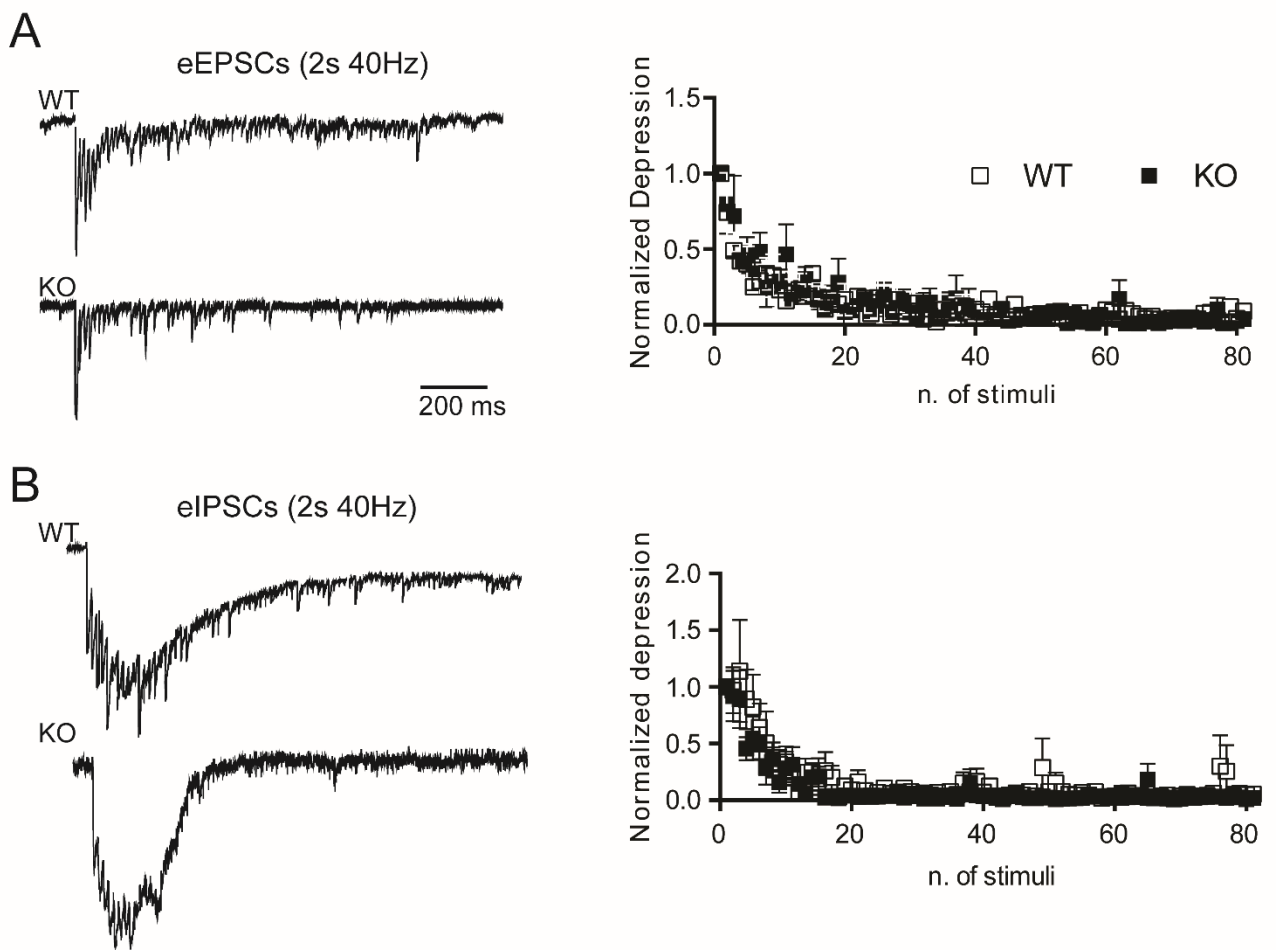


Figure S8